Accepted Manuscript

Quantification of source specific black carbon scavenging using an aethalometer and a disdrometer

C. Blanco-Alegre, A.I. Calvo, E. Coz, A. Castro, F. Oduber, A.S.H. Prévôt, G. Močnik, R. Fraile

PII: S0269-7491(18)33445-6

DOI: https://doi.org/10.1016/j.envpol.2018.11.102

Reference: ENPO 11929

To appear in: *Environmental Pollution*

Received Date: 27 July 2018

Revised Date: 22 October 2018

Accepted Date: 29 November 2018

Please cite this article as: Blanco-Alegre, C., Calvo, A.I., Coz, E., Castro, A., Oduber, F., Prévôt, A.S.H., Močnik, G., Fraile, R., Quantification of source specific black carbon scavenging using an aethalometer and a disdrometer, *Environmental Pollution* (2018), doi: https://doi.org/10.1016/j.envpol.2018.11.102.

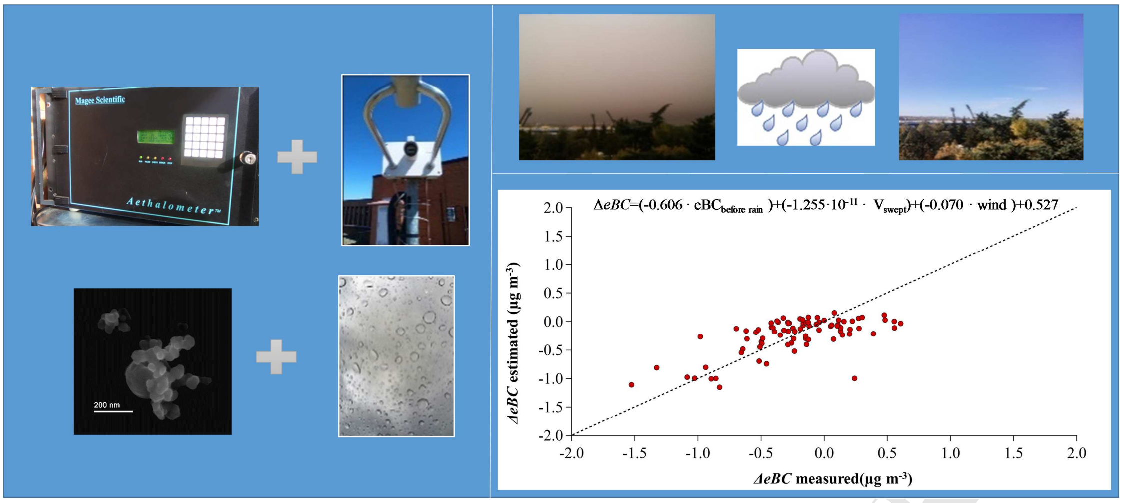
Magee Scientific
Aethalometer
200 nm
ΔeBC=(-0.606 · eBC_before rain)+(-1.255·10^-11 · V_swept)+(-0.070 · wind)+0.527
ΔeBC estimated (µg m^-3)
ΔeBC measured(µg m^-3)
2.0
1.5
1.0
0.5
0.0
-0.5
-1.0
-1.5
-2.0

Quantification of source specific black carbon scavenging using an aethalometer and a disdrometer

C. Blanco-Alegre [(1)], A.I. Calvo [(1)], E. Coz [(2)], A. Castro [(1)], F. Oduber [(1)], A.S.H. Prévôt [(3)], G. Močnik [(4)], R. Fraile [(1)]

[(1)] *Department of Physics, IMARENAB University of León, 24071 León, Spain*
[(2)] *Centre for Energy, Environment and Technology Research (CIEMAT), Department of the Environment, Madrid, Spain*
[(3)] *Laboratory of Atmospheric Chemistry, Paul Scherrer Institute, 5232 Villigen, Switzerland*
[(4)] *Condensed Matter Physics Dept., Jožef Stefan Institute, 1000 Ljubljana, Slovenia*

Corresponding Author: roberto.fraile@unileon.es *+34987291543*

ABSTRACT

Aerosol black carbon (BC) is the second strongest contributor to global warming, after CO_2, and it is linked to many adverse health effects. A sampling campaign of 15 months was carried out in León (Spain) in order to evaluate the scavenging of BC with an ensemble aethalometer-disdrometer. The aethalometer provides the concentration of equivalent black carbon (eBC), and the disdrometer, the raindrop size distribution. A total of seventy-five rain events were studied and in 73% of them there was an effective ($eBC_{initial} > eBC_{final}$) scavenging, with a mean decrease of $48 \pm 37\%$ in long rain events (>8 h) and $39 \pm 38\%$ in short rain events. The scavenging of BC is strongly related to its source. Thus, the scavenging coefficient (*SC*) mean value of the BC from fossil fuel (eBC_{ff}) for short and long rain events was $5.1\ 10^{-5}$ and $1.3\ 10^{-5}\ s^{-1}$, respectively. For the BC from biomass burning (eBC_{bb}), the *SC* values were $1.6\ 10^{-4}$ and $2.8\ 10^{-5}\ s^{-1}$ in short and long events, respectively. There was a significant positive correlation between the *SC* and the number of drops with diameters between 0.375 and 2.5 mm. Rain scavenging of eBC was analyzed depending on the air mass origin obtaining an effective scavenging for air masses from Atlantic, Arctic and Africa. A linear model (R^2=0.72) was built to estimate the *ΔeBC* values with variables from an aethalometer, a disdrometer and a weather station: eBC concentration before rain, swept volume and precipitation accumulated. A Kolmogorov-Smirnov statistical test confirmed the goodness of fit of the model to the measured data.

KEYWORDS: Black carbon, BC scavenging estimation model, raindrop diameter, rainfall, scavenging coefficient, wet deposition.

CAPSULE:
The combination of aethalometer and disdrometer measurements reveals that the scavenging of BC depends strongly on the BC source (biomass burning or fossil fuel combustion).

1. INTRODUCTION

Atmospheric aerosols, both natural and anthropogenic, affect human health (Apte et al., 2015; Fröhlich-Nowoisky et al., 2016; HEI Review Panel, 2013; Pöschl, 2005; WHO, 2007) and climatic change because of the significant contribution to the Earth's radiation budget either directly and indirectly (Andreae and Ramanathan, 2013; ICCP, 2014; Menon et al., 2002; Pöschl, 2005). In Europe, more than 90% of city dwellers are exposed to $PM_{2.5}$ levels that exceed the reference value set by WHO (EEA, 2013).

One of the major atmospheric aerosol pollutants is black carbon (BC) which is emitted during incomplete combustion of fossil fuel or biomass. It is a carbonaceous material formed primarily in flames and directly emitted to the atmosphere, with some particular physical properties: it strongly absorbs visible light and is refractory with a vaporization temperature of around 3700 °C (Bond et al., 2013). It is noteworthy that BC particles are insoluble in water and organic solvents and, therefore, they are not scavenged directly from the atmosphere due to wet deposition (AMAP, 2011). Some studies (e.g. Granat et al., 2010) indicate that BC keeps its hydrophobic property even after being in the atmosphere for several days. However, the BC morphology (organized as fractal-like aggregates) facilitates sorption of other species (Petzold et al., 2013) and it becomes hydrophilic and accessible for wet deposition. The BC cycle is controlled by emissions, transport and deposition. Among these factors, wet deposition is the most complex (Mori et al., 2014).

According to Bond et al., (2013), the main sources of BC are: i) diesel engines used for transport, ii) residential solid fuels (wood and coal), iii) forest fires, and iv) industrial processes. In these burning processes, small carbon spherules are formed, with diameters between 10 and 50 nm and, subsequently, accumulated in aggregates. This aggregates formation starts at or shortly after emission and the aggregates get internally or externally mixed. Their size distribution depends on the formation mechanism and atmospheric processes during transport, while they grow via coagulation. Regarding to aggregate sizes, these particles belong to the Aitken mode (30-100 nm) but due to subsequent coagulation and condensation of inorganic and organic secondary molecules, they can grow to sizes in the accumulation mode (100-1000 nm) (Conrady et al., 2013).

BC also plays an important role in the environment, for example in the formation of acid precipitation through the catalytic oxidation of sulfur dioxide to sulfate (Novakov, 1984; Singh et al., 2016). The main BC aerosol effect on climate is due to the strong ability to absorb solar radiation. The impact of BC on climate change remains largely uncertain (Hienola et al., 2013). Nevertheless, the global mean radiative forcing caused by BC was estimated to be from 0.4 to 1.2 W m^{-2}, becoming the second strongest contributor to global warming, after CO_2 (Bond et al., 2013; ICCP, 2014). Several studies (AMAP, 2011; Righi et al., 2011) have found that BC affects the Earth's radiation budget in three different ways: i) aerosol direct effect (absorption or scattering of shortwave radiation), ii) aerosol indirect effect (interaction with clouds) and iii) semi-direct effects (BC deposition to ice/snow enhances the absorption of shortwave radiation inducing melting process).

BC may be a pollutant toxic to human health, linked to many illnesses: respiratory (such as adverse effects on lung function and increase cancer risks) and cardiovascular diseases (Janssen et al., 2011; WHO, 2012), and it causes an increase in population morbidity and mortality (Silverman et al., 2012; Suglia et al., 2008), mainly affecting the children's health (UNICEF, 2016) (due to the immature host defense system) and people with chronic respiratory diseases

(Jansen et al., 2005). The set of BC and organic carbon is estimated that producing annually around 3 million premature deaths (Apte et al., 2015; Bond et al., 2013; Lelieveld et al., 2015; WHO, 2012). Hence, the study of black carbon concentration is crucial due to its effects on multiple essential policy objectives like climate, air quality or public health (EEA, 2016; Font and Fuller, 2016; Kinney, 2008; Tong et al., 2017, 2016).

To measure BC, the use of aethalometer (Hansen et al., 1984) has been common in last years. The aethalometer provides the concentration of equivalent black carbon (eBC) (carbon mass derived from the light attenuation coefficient). The multi-wavelength aethalometer data may be used to separate the fossil fuel (eBC_{ff}) and the biomass burning (eBC_{bb}) contributions to eBC through the "aethalometer model" (Becerril-Valle et al., 2017; Harrison et al., 2013; Sandradewi et al., 2008b; Zotter et al., 2017).

Wet and dry deposition is the only important sink of BC, due to its stability. The atmospheric lifetime of BC aerosols ranges from days to weeks depending on the local meteorology (Begam et al., 2016). Dry deposition is able to eliminate larger particles in several days, and sub-micron fraction in several weeks, hence this is a slow process. However, observations have shown that wet deposition represents 70–85% of the tropospheric sink for the carbonaceous aerosols (Pöschl, 2005). Therefore, wet deposition is the main process to mitigate the effects of BC on the climate, human health and ecosystems (Cerqueira et al., 2010) in a brief lapse of time, but this process is not yet well explored. Wet deposition is considered one of the most uncertain processes in models (Textor et al., 2006).

Below-cloud scavenging (BCS) linked to wet deposition, constitutes an important sink of aerosol particles, including BC (Chate, 2005; Latha et al., 2005; Sportisse, 2007; Tost et al., 2006; Zhao et al., 2015). However, the study of BC aerosol-precipitation interaction does not constitute an easy task. The complexity in the characterization of BCS lies in the dependence on several parameters, for example concentration, chemical composition or electric charges (Ladino et al., 2011). Many researchers have tried to quantify the wet scavenging effect on aerosols and gases (Chate et al., 2003; Laakso et al., 2003; Maria and Russell, 2005; Olszowski, 2015), but there are few studies on BC scavenging by rainfall to date. Furthermore, most of them are based on the determination of elemental carbon (EC) concentration by thermo-optical methods (Armalis, 1999; Budhavant et al., 2016; Cerqueira et al., 2010; Custódio et al., 2014; Granat et al., 2010). These studies are carried out in time intervals (sampling period of one day or several hours) that are long compared to the rain event duration. A simultaneous and continuous study of BC concentration and raindrop sizes would provide a deeper knowledge about the BC-precipitation interaction.

A 15 months sampling campaign for measuring BC concentration (with an aethalometer) and raindrop physical characteristics (with a disdrometer) has been carried out in León (NW Spain). An estimation of below-cloud scavenging on BC according to rainfall characteristics and origin of air masses has also been accomplished. As far as we know, this type of studies is unprecedented.

2. MATERIAL AND METHODS

2.1. Sampling site and measurements

The sampling site is located in the campus of the University of León (Fig. S1), a city situated in the NW of the Iberian Peninsula (42° 36′ N, 05° 35′ W) at 838 m above sea level and with a population of about 200,000 including the metropolitan area. According to Oduber et al. (2018) the main source of particulate emissions is traffic and domestic heating, due to the absence of large emitting industries. It is worth noting that, nowadays, the use of coal combustion in heating devices is still usual in León. León features a Mediterranean climate with continental features and tempered by the proximity of the Cantabrian Mountain Range with an annual mean precipitation of 515 mm (Castro et al., 2010).

The sampling was carried out between 12 February 2016 and 31 August 2017 (except spring 2017, due to technical issues). The instruments were located on the terrace of the Faculty of Veterinary Medicine of the University of Léon.

The following season distribution along the year was considered: winter from 15 December to 14 March, spring from 15 March to 14 June, summer from 15 June to 14 September and autumn from 15 September to 14 December.

2.2. Black carbon data

An aethalometer model AE-31 (Magee Scientific, USA) with a time resolution of 2 minutes and a precision of 10^{-3} µg m^{-3} was used for BC concentration determination. It continuously measures attenuation of light due to the deposition of ambient aerosol on the instrument's filter tape at seven wavelengths: 370, 470, 520, 590, 660, 880 and 950 nm. The sample flow rate was set to be 4 L min^{-1} and verified with Gilibrator measurements. To determine the eBC concentration in the sampled air, the aethalometer uses a differential radiometric optical transmission technique. The instrument operation was described in detail by Hansen (2005) and Virkkula et al. (2007).

In order to avoid possible bias in measurements due to the fast changes in relative humidity, the aethalometer data recorded during rain was not taken into account: only data before and after rain were considered. To decrease uncertainties derived from detector response, instrumental noise, flow rate and filter spot area (Corrigan et al., 2006), the 2-min eBC data has been averaged at a resolution of 1 h, comparable to the rain events duration.

The contribution from fossil fuel (eBC_{ff}) and biomass burning (eBC_{bb}) was estimated through the application of the aethalometer model (Sandradewi et al., 2008a). Likewise, hourly eBC, eBC_{ff}, eBC_{bb} concentrations and Absorption Ångström Exponent (AAE) were determined. Light absorption measurements at λ_1=470 nm and λ_2=950 nm (Becerril-Valle et al., 2017; Harrison et al., 2013; Sandradewi et al., 2008b) have been used in this work ($\mathrm{AAE}(\lambda_1,\lambda_2) = -\frac{\ln(b_{abs}(\lambda_1)/b_{abs}(\lambda_2))}{\ln(\lambda_1/\lambda_2)}$). To obtain the AAE values, the shorter wavelength of 470 nm has been used rather than the 370 nm one, because the latter is influenced by the varying presence of secondary organic aerosol (SOA) with highly variable optical properties (Zotter et al., 2017). The source specific AAE values used in the aethalometer model to estimate the biomass burning and fossil fuel contributions are AAE_{bb}=1.68, according to Zotter et al. (2017) and AAE_{ff}=0.95 derived from measurements in a traffic hotspot in the León center in May during morning rush hours. The mean temperatures were high, so traffic can be considered like the only source at this point. In Supplementary material, the Aethalometer model equations are shown.

The AAE values below 0.7 and above 4 (less than 2% along the sampling) were eliminated from the database because these measurements could be affected by instrumental noise, detector response or meteorological conditions (Corrigan et al., 2006).

The eBC data recorded during the sampling period were treated following Aerosol, Clouds, and Trace gases Research InfraStructure Network (ACTRIS) guidelines (Virkkula et al., 2007).

2.3. Disdrometer and meteorological data

The raindrop size spectrum has been obtained using a disdrometer, Laser Precipitation Monitor (LPM) of *Thies Clima*, which registered drops between 0.125 and 8 mm in 21 drop size ranges. A detailed description can be found in Fernández-Raga et al. (2009). From the data provided by the LPM, the following rainfall variables were obtained every minute: precipitation intensity, accumulated precipitation, number of drops in 21 channels, volume swept by falling drops (mm^{-3} m^{-3}), mean and standard deviation of raindrop sizes. The 1-min data have been averaged at a resolution of 1 h, like eBC data.

Next to disdrometer, a weather station was installed for continuously registering the temperature, humidity, wind intensity and direction. Univariate analysis (i.e. mean, median, minimum, maximum, quartiles and standard deviation) was used to calculate hourly BC concentration, rainfall variables and meteorological data.

2.4. Air mass trajectories

Through the application of HYSPLIT4 (Hybrid Single Particle Lagrangian Integrated Trajectory) (Draxler and Rolph, 2012) the air masses trajectories were analyzed in order to determine sources and origin of the air masses present in León during rain events. This model was used to compute four-days back trajectories at every rain event, at arrival altitudes of 500 and 1000 m a.g.l. over León (Custódio et al., 2014). The average altitude of 1000 m is representative of the diurnal mixing layer thickness at León (Calles et al., 2018).

The model was run with meteorological data from the Global Data Assimilation System (GDAS) archives (http://ready.arl.noaa.gov/HYSPLIT_traj.php).

Based on back trajectories at 1000 m a.g.l. over sampling point, a six groups classification of the prevailing air mass origin and transport pathway have been made. The group assigned coincides with the sector on which the air mass spent most of the time. The regions (Fig. S2) are:

- Group I: Arctic
- Group II: Atlantic
- Group III: Continental
- Group IV: North America
- Group V: North Atlantic
- Group VI: Saharan

Besides, a Circulation Weather Types (CWTs) classification was carried out based on Lamb (1972), to identify the type of weather related with a specific synoptic situation. This method has been previously used in the Iberian Peninsula (Calvo et al., 2012; Russo et al., 2014). The direction and vorticity of the geostrophic flow, obtained for 16 grid points distributed over the Iberian Peninsula (Trigo and DaCamara, 2000), have been used to establish each of the 26 different CWTs. Eight weather types are identified as “pure” and are characterized by a specific predominant wind component, regardless of their intensity: N, S, E, W, NW, SW, SE and NE. Other two of them are the so-called “non-directional”: anticyclonic (A) and cyclonic (C). As a result of the combination of “non-directional” with “pure” types, other 16 CWTs, so-called “hybrid” types, are obtained. A detailed explication of this classification may be found in Trigo and DaCamara (2000).

2.5. Selecting data criteria

The rain events considered in this study are those that fulfill the following conditions:

a) an accumulated precipitation greater than 0.2 mm was registered in one hour (minimum rain amount considered significant),
b) there was a minimum of 2 h without rain between events,
c) there were eBC and eBC_{ff} concentrations greater than 0.5 µg m^{-3} and greater than 0.1 µg m^{-3} for eBC_{bb},
d) rain duration was shorter than 24 h.
e) a maximum difference of 2 m s^{-1} in wind speed and 50° in wind direction during rain event has been registered (Kyrö et al., 2009; Paramonov et al., 2011) to avoid changes in eBC concentration due to advection (Laakso et al., 2003).

Furthermore, in order to minimize the eventual interference of coal combustion in the eBC_{bb} estimated by the Aethalometer model, the events in which coal combustion tracers (As and Se) (Vejahati et al., 2010; Wang et al., 2018) were registered, have been removed from eBC_{bb} analysis. Levoglucosan (biomass burning tracer (Gonçalves et al., 2011)) or ^{14}C measurements (as in Zotter et al. 2017) were not available.

For each rain event, the eBC, eBC_{ff} and eBC_{bb} concentration one hour before and one hour after precipitation have been analyzed. In order to determine the eBC concentration change between time intervals t_1 and t_2, with eBC concentrations c_1 and c_2, respectively, the following parameter was calculated:

$$\Delta eBC_{rel} = -100\frac{\Delta eBC}{c_1} \tag{1}$$

where $\Delta eBC = c_2 - c_1$ and the minus sign before 100 has been introduced in order to get a positive value of ΔeBC_{rel} when the eBC concentration decreases (effective scavenging). Furthermore, for a group of events, a new parameter has been defined as the concentration-weighted average $\left(\Delta eBC\% = \frac{\sum(\Delta eBC_{rel} \cdot c_1)}{\sum c_1}\right)$.

A global analysis of all the events that meet the previously cited requirements was carried out. The average length of rain events in León was 3:28 h with a standard deviation of 4:07 h. The episodes of extreme duration could be referred to as “long events”. A possible quantification may be the 10 % of the total events or the average plus one standard deviation. Both criteria conducted to the same threshold of about 8 hours. Consequently, events exceeding 8 h were called long events, and the rest short events.

The equation used to estimate eBC scavenging coefficient, was the same often used to calculate scavenging coefficient (*SC*) from the concentration change *c* of aerosol particles and other elements like sulphates (Chate et al., 2003; Laakso et al., 2003; Maria and Russell, 2005; Olszowski, 2015). In this study, *c* is the eBC concentration. The scavenging coefficient *SC* (s^{-1}) is defined as a rate of aerosols washout by precipitation.

$$SC = -\frac{1}{c}\cdot\frac{dc}{dt} \tag{2}$$

The integration of this equation between t_1 and t_2 with concentrations c_1 and c_2 gives:

$$SC = -\frac{1}{t_1 - t_2} \cdot \ln \frac{c_2}{c_1} \tag{3}$$

The scavenging coefficient *SC* varies with collection efficiency, particles and raindrop size distributions and their terminal velocities, for different particle sizes (Seinfeld and Pandis, 2006). Although the scavenging coefficient is usually called λ, it is represented in this study by *SC*, as λ refers here to wavelength.

When speaking about an effective scavenging, we will refer to the positive values of $\Delta eBC\%$ and *SC*. This decrease of the BC concentration can also be influenced by vertical mixing changes or even by advection.

2.6. Diurnal pattern normalization

We eliminated the important effect of the diurnal cycle on the eBC, eBC_{ff} and eBC_{bb} concentrations by normalizing the daily concentrations to the daily average. For no-rain days during the sampling period, daily patterns of eBC, eBC_{ff} and eBC_{bb} hourly concentration were obtained. The eBC concentration of all days without rain between March 2016 and August 2017 were used and the seasonal daily patterns were calculated in the following way: first of all, for each day, the ratio between the hourly eBC concentration and the mean eBC concentration of that day was calculated. With the daily normalized values, the average diurnal pattern was determined. In other words, we have calculated the hourly ratio ($R_{i,j}$) of the diurnal pattern for the hour *i* of the day *j* through the following formula:

$$R_{i,j} = \frac{c_{i,j}}{\bar{c}_j} \tag{4}$$

where $\bar{c}_j = \frac{\sum_i c_{i,j}}{n}$, *n* being the number of hours in one day (24). We have subsequently determined the average R_i mean for each season:

$$R_i = \frac{\sum_j R_{i,j}}{d} \tag{5}$$

d being the number of complete sampling days without rain for each season (22, 52, 81, 70, 81 and 62 days for winter 2016, spring 2016, summer 2016, autumn 2016, winter 2017 and summer 2017, respectively).

3. RESULTS AND DISCUSSION

The seasonal eBC values in León, during sampling are presented in Table S1. eBC_{ff} values registered during autumn 2016 and winter 2017 are higher probably due to the increase in road traffic and the use of heating devices. In all seasons, there were two peaks throughout the day (0600-0800 and 1600-2000 UTC), mainly during rush hours' traffic (Fig. S3). In the afternoons, heating emissions add to the afternoon peak. Likewise, eBC_{bb} values in winter and autumn were higher, because of the use of biomass for heating. Other cities like Beijing, Leicester, Hefei or Kadapa, have shown the same pattern (Begam et al., 2016; Cheng et al., 2014; Hama et al., 2017; Zhang et al., 2015, 2017) caused by traffic and domestic heating.

3.1. Rain effect on equivalent black carbon concentration

Seventy-five rain events were observed during the sampling period. The rain events are concentrated in winter and spring, showing a clear decrease in summer (Fig. S4).

3.1.1. Rain events characteristics

The main characteristics of short and long events are shown in Table 1. Seven long events were observed during the sampling period. There was an effective eBC scavenging in 6 events (86% of total), with a mean decrease of 48 ± 37%. Long events featured the mean raindrop diameter of 0.34 ± 0.19 mm, with a mean swept volume per event of 1.9 10^{10} mm^3 m^{-3} and a mean number of drops of 8.8 10^7 m^{-2}. Of the 75 events registered, 68 rain events were short. There was an effective eBC scavenging in 49 of the short events (73% of total), with a mean decrease of 39 ± 38%. The mean raindrop diameter for short events was 0.34 ± 0.20 mm, with a mean swept volume per event of 2.5 10^9 mm^3 m^{-3} and a mean number of drops of 9.0 10^6 m^{-2}.

The decrease in eBC_{bb} concentration in both short and long events is significantly higher compared to eBC_{ff}. This fact is probably due to the higher fraction of organics from biomass burning, and also a higher degree of oxygenation (O:C) of biomass burning organic aerosol compared to traffic organic aerosol, thus increasing its hydrophilic property (Cerully et al., 2011; Safai et al., 2014; Zheng et al., 2017). In addition, the size including the organics for wood burning being larger than for traffic emissions may play a role (Blanco-Alegre et al., 2018). Following the criteria given in section 2.5 (more specifically, the criterium c), the events considered to determine the eBC, eBC_{ff} and eBC_{bb} values were different. Therefore, the eBC value may not lie between the eBC_{ff} and eBC_{bb} specific ones.

Table 1. Number of rain events (*N*), percentage of rain events with effective scavenging (% of events) and mean decrease (and standard deviation) in BC concentration (*ΔeBC%*).

	Short events (< 8 h)			Long events (> 8 h)		
	N	% of events	*ΔeBC%*	*N*	% of events	*ΔeBC%*
eBC	68	73	39 ± 38	7	86	48 ± 37
eBC_{ff}	60	75	40 ± 33	7	71	46 ± 30
eBC_{bb}	27	85	75 ± 46	3	67	96 ± 5

3.1.2. Extreme scavenging events

According to the scavenging efficiency, a classification of rain events in three groups has been carried out: type I (ΔeBC_{rel} higher than 50%), type II (ΔeBC_{rel} between 0-50%) and type III (non-effective scavenging) (Table 2). It can be seen that events with more effective scavenging were characterized by: i) a longer duration of events, ii) a greater precipitation accumulated and iii) a higher wind intensity. The events with no scavenging effect featured somewhat lower eBC concentration before rain. However, there were no major differences in the rainfall parameters analyzed between types II and III.

Table 2. Mean and standard deviation values of rain parameters for the three types of events stablished according to the scavenging efficiencies.

	N	Duration (h:min)	Rain (mm)	Rainfall intensity (mm h^{-1})	Wind speed (m s^{-1})	Raindrop diameter (mm)	eBC before rain (μg m^{-3})	Swept volume (mm^3 m^{-3})
Type I (ΔeBC_{rel} >50%)	18	4:24 ± 3:30	8.2 ± 12.5	1.2 ± 1.3	1.9 ± 1.3	0.31 ± 0.09	1.1 ± 0.7	9.6 10^9
Type II (ΔeBC_{rel} 0-50%)	39	2:47 ± 2:32	2.4 ± 3.4	0.7 ± 0.8	1.1 ± 1.3	0.36 ± 0.09	1.1 ± 0.5	3.0 10^9
Type III (ΔeBC_{rel} <0%)	15	2:36 ± 2:08	1.8 ± 3.0	0.5 ± 0.4	1.2 ± 1.0	0.35 ± 0.06	0.9 ± 0.4	2.9 10^9

The event with the highest scavenging efficiency occurred on 21st March 2017 with an accumulated rainfall of 3.05 mm and a mean rainfall intensity of 0.57 mm h^{-1}. The maximum intensity was 0.05 mm min^{-1}. The rain started at 0800 UTC and lasted 228 min. The eBC concentration was 2.62 μg m^{-3} and 0.22 μg m^{-3} two hours before and two hours after rain, respectively (ΔeBC_{rel} = 88%). The mean raindrop size was 0.44 ± 0.22 mm and the mode of raindrop size was 0.31 mm. The swept volume was 6.2 10^9 mm^{-3} m^{-3}.

On the other hand, the event with the highest eBC percentage increase occurred on 24th February 2016 with an accumulated rainfall of 1.92 mm and a mean rainfall intensity of 3.96 mm h^{-1}. The maximum intensity was 0.06 mm min^{-1}. A eBC increase was registered, with 1.33 μg m^{-3} and 1.98 μg m^{-3} two hours before and two hours after rain, respectively (ΔeBC_{rel} = -34%). The rain started at 1149 UTC and lasted 173 min. The mean raindrop size was 0.32 ± 0.19 mm and the mode of raindrop sizes was 0.27 mm. The swept volume was 2.8 10^9 mm^{-3} m^{-3}. An explanation could be the change from a deep mixing layer to a shallow one, as proposed by Talukdar et al. (2015) for Calcutta. Thus, the change in surface and air temperature reduced the mixing layer height and the eBC concentration increased.

Besides, another contribution to the differences in scavenging efficiency may be the higher swept volume recorded in the event with effective scavenging, caused by a longer event duration and a higher raindrop diameter.

3.2. Air masses origin and weather types

The four-days back trajectories of air masses arriving in León at 1000 m a.g.l. were obtained from HYSPLIT model. In Fig. S5 the seasonal back trajectories for rain events are shown.

The main origins of air masses during rain events were Atlantic (33%), Continental (20%) and North Atlantic (19%) (Table S2). In winter 2017, there was a prevalence of air mass coming from North Atlantic (56%), and in summer 2017 there was a high frequency of air masses with Saharan origin (56%). The highest values of eBC concentrations were recorded in air masses coming from North America (during winter 2017) and in intrusions from Sahara (during summer 2017). No significant statistical differences were observed in eBC concentration between air masses during rainy days.

The air masses presented the following effective ($eBC_{initial}$ > eBC_{final}) scavenging values: Arctic (29 ± 21%), North Atlantic (35 ± 31%) and Saharan (18 ± 21%). However, Continental (6 ± 39%), North America (6 ± 7%) and Atlantic (4 ± 39%) masses present a lower mean eBC decrease (Table S3), maybe due to the high eBC load transported by these air masses.

The most frequent weather types during rain events were C (23 cases) and NW (9 cases). There was a decrease in eBC concentration in all the weather types except for NE and AS. NE type is noteworthy, since it comprises many events. The two AS events were characterized by a stagnation of the air mass coming from Sahara. On the other hand, during NW rain events (9 cases), a *ΔeBC%* of 45% was registered. Other weather types with W component, like W, SW, ANW, CW and AW present a clear decrease (Table S3). Figure 1 shows the *ΔeBC%* regarding the origin of air (according to Weather Lamb type). There was an effective scavenging in all components except NE, indicative of an eBC source in these directions. This increase coincides with that observed in Continental masses based on HYSPLIT trajectories.

During rain events of pure anticyclonic type, there was an increase in eBC concentration of 27%, and a mean raindrop diameter of 0.30 ± 0.09 mm. On the contrary, when the type was pure cyclonic, a decrease in eBC concentration of 1% was recorded, with a mean raindrop diameter of 0.36 ± 0.07 mm.

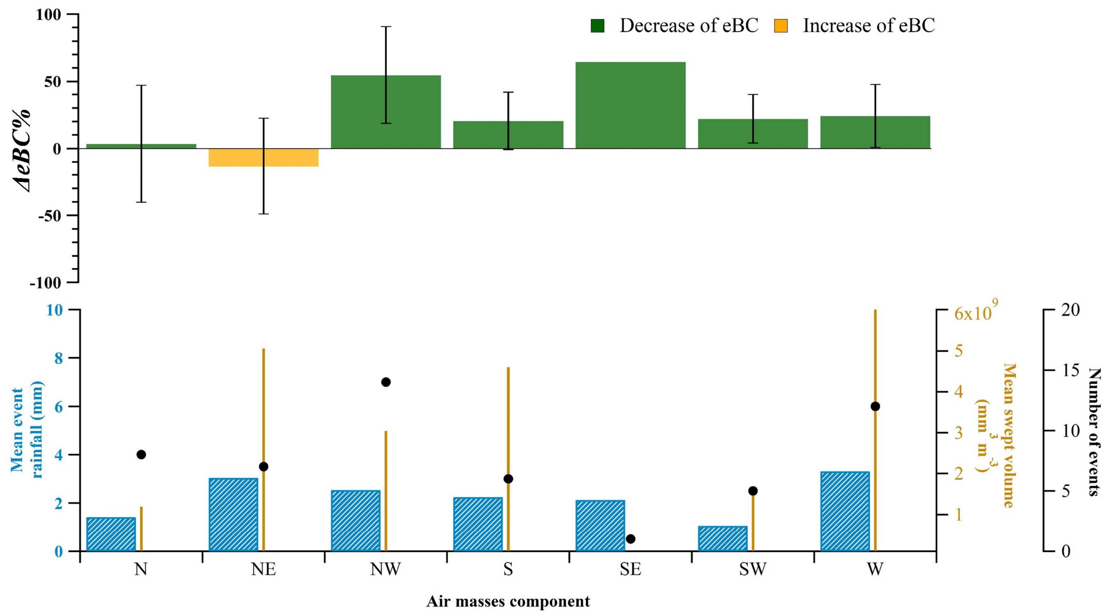

Fig. 1. *ΔeBC%* between before and after rain according to air mass origin of Circulation Weather Types (CWTs) during rain events. Black dots indicate the number of rain events, striped boxes indicate the mean rainfall (mm) and vertical lines indicate the mean swept (mm^3 m^{-3}) per event.

3.3. Scavenging coefficients

During the 68 rain short events (with a mean intensity of 0.82 mm h^{-1}), *SC* for eBC showed a mean value of 4.7 10^{-5} s^{-1} (with a standard deviation of 8.4 10^{-5} s^{-1}) and a median of 4.0 10^{-5} s^{-1} (interquartile range: -8.8 10^{-6} to 7.92 10^{-5} s^{-1}). Positive values of *SC* are indicative of effective scavenging (Table 3).

In the 7 rain long events (with a mean intensity of 1.42 mm h^{-1}), *SC* for eBC indicated a mean value of 1.0 10^{-5} s^{-1} (with a standard deviation of 1.1 10^{-5} s^{-1}) and a median of 1.1 10^{-5} s^{-1} (interquartile range: 3.7 10^{-6} to 1.9 10^{-5} s^{-1}). It should be noted that *SC* for eBC_{bb} in short events was around three to four times higher than *SC* of eBC and eBC_{ff}. The *SC* for eBC in short events was about four times the value obtained for long events. However, *ΔeBC%* was greater in long events (Table 1). Thus, the greater decreased in long events may be caused by the great long duration of events. To estimate the effect of rain duration on the *ΔeBC%*, the correlation between both variables was analyzed. A correlation coefficient R^2 of 0.14 was obtained, which means that the rain duration explains a 14% of the total variance of *ΔeBC%*.

Table 3. Scavenging coefficients (*SC*) in s^{-1} of eBC, eBC_{ff} and eBC_{bb} in short and long events. Number of events are in brackets.

	SHORT EVENTS (68)			LONG EVENTS (7)		
	SC (eBC) (68)	*SC* (eBC_{ff}) (68)	*SC* (eBC_{bb}) (27)	*SC* (eBC) (7)	*SC* (eBC_{ff}) (7)	*SC* (eBC_{bb}) (3)
Min	$-1.3\ 10^{-4}$	$-1.0\ 10^{-4}$	$-8.0\ 10^{-5}$	$-6.7\ 10^{-6}$	$-6.6\ 10^{-6}$	$-9.5\ 10^{-6}$
Q1	$-8.8\ 10^{-6}$	$-9.2\ 10^{-6}$	$2.2\ 10^{-6}$	$3.7\ 10^{-6}$	$-3.4\ 10^{-5}$	$1.1\ 10^{-5}$
Median	$4.0\ 10^{-5}$	$3.2\ 10^{-5}$	$6.6\ 10^{-5}$	$1.1\ 10^{-5}$	$1.3\ 10^{-5}$	$3.1\ 10^{-5}$
Q3	$7.9\ 10^{-5}$	$9.4\ 10^{-5}$	$2.5\ 10^{-4}$	$1.9\ 10^{-5}$	$2.9\ 10^{-5}$	$4.7\ 10^{-5}$
Max	$2.5\ 10^{-4}$	$2.8\ 10^{-4}$	$1.1\ 10^{-3}$	$2.3\ 10^{-5}$	$3.4\ 10^{-5}$	$6.4\ 10^{-5}$
Mean	$4.7\ 10^{-5}$	$5.1\ 10^{-5}$	$1.6\ 10^{-4}$	$1.0\ 10^{-5}$	$1.3\ 10^{-5}$	$2.8\ 10^{-5}$
Desvest	$8.4\ 10^{-5}$	$8.5\ 10^{-5}$	$2.6\ 10^{-4}$	$1.1\ 10^{-5}$	$1.8\ 10^{-5}$	$3.7\ 10^{-5}$

Current information on BC scavenging ratios available in the literature is still scarce. Nevertheless, the values obtained were similar to those indicated by Latha et al. (2005) ($1.64\ 10^{-5}$ s^{-1}) in India, although their value was obtained using a different method. The observed differences could be due to the lower BC concentrations in León (8 times lower than in its location, Hyderabad and Secunderabad, India).

A global analysis of rain events gives positive values of *SC* for eBC (indicative of an effective scavenging), higher for short events. Furthermore, these *SC* values are in the same order of magnitude that those obtained in other studies about fine and ultrafine aerosols (Laakso et al., 2003; Zikova and Zdimal, 2016).

3.4. Relation between *SC* and meteorological parameters

For each rain event, the *SC* value has been related to the wind intensity and the rainfall intensity in order to observe the influence of these meteorological variables on eBC concentration. In Fig. 2, it can be observed that most of the events presented positive values (effective scavenging). The rain events with intensities greater than 2 mm h^{-1} were scarce but they always presented an effective eBC scavenging. Events with rain intensities less than 2 mm h^{-1} caused an effective eBC scavenging in 70% of cases.

It should be noted that there was no clear influence of the wind speed during rain, although in the events with no effective scavenging, low wind speed dominated. Nevertheless, the wind and the eBC concentration two hours before rain presented a statistically significant negative correlation. The wind causes a higher dispersion of eBC, hindering the scavenging by rain.

There was a statistically significant negative correlation between event duration and ΔeBC_{rel}. This supports the influence of rain duration over eBC concentration (see Fig. S6). Other studies have also shown that low intensities and large duration of rain events produce a higher effective scavenging (Chatterjee et al., 2012). Besides, vertical mixing and horizontal advection could also be related with ΔeBC (Joshi et al., 2016), mainly in autumn and winter.

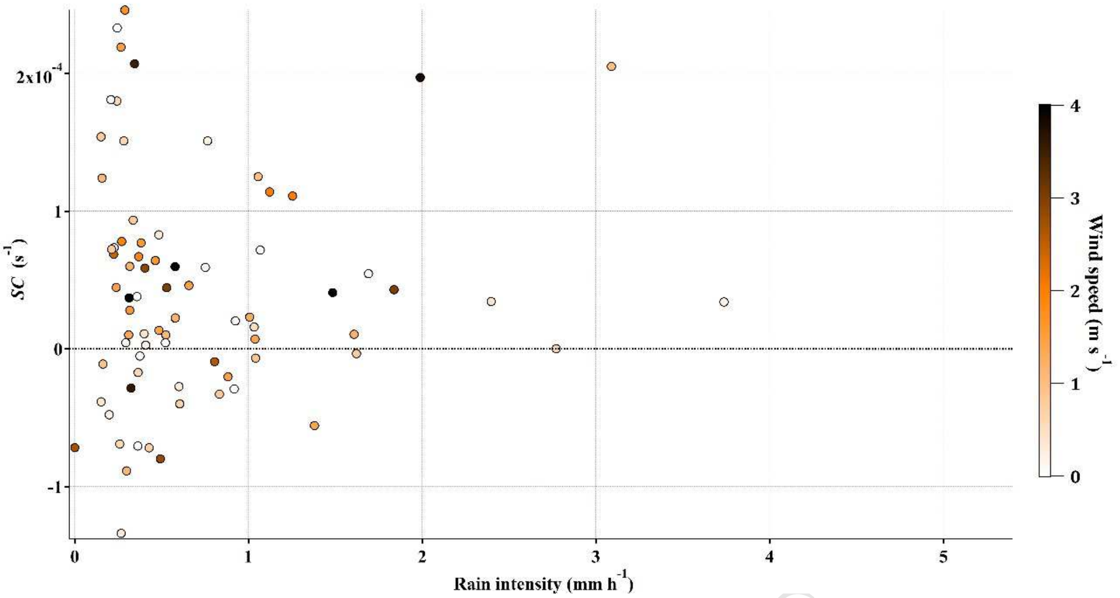

Fig. 2. Relationship between black carbon scavenging coefficients (*SC*) and rainfall intensity. Wind speed is indicated by the colour scale inside the dots.

3.5. Model for *ΔeBC*

To parameterize the *ΔeBC*, a linear model has been built using aethalometer and disdrometer variables. What variables can be the most appropriate to build this model? Previously, the correlations between *ΔeBC* and variables like wind speed, eBC concentration before rain, event duration, precipitation accumulated, mean rainfall intensity, mean raindrop diameter and sum of volume swept by falling drops have already been analyzed. Furthermore, the raindrop size could also be connected to *ΔeBC*. In fact, the data obtained from 21 drop size ranges of LPM (between 0.125 and 8 mm) have been used to check the relationship between the number of raindrops in each size channel and the *SC* in events with efficient scavenging (Table S4). As a result, a significant correlation between the *SC* and the number of drops with diameters between 0.375 and 2.5 mm has been found. The rest of the raindrop diameters did not present significant correlations with *SC*.

Consequently, the variables tested to build the model have been the following: wind speed, eBC concentration before rain, event duration, precipitation accumulated, mean rainfall intensity, mean raindrop diameter, change in the mixing layer height, sum of volume swept by falling drops and number of drops with diameters between 0.375 and 2.5 mm. Besides, we have included two variables related to the mixing layer height that could affect the rain scavenging: the mean height during rain and the change in height throughout the rain event. The application of an automatic linear modelling (IBM SPSS Statistics 24) by stepwise, with an entry probability of 0.05 and removal probability of 0.10 has been used.

With this methodology, a model has been built from a random sample including the 75% of the total data set. This model has been applied to the remaining 25%. Subsequently, a Kolmogorov-Smirnov statistical test has been carried out in order to check the goodness of fit of the model to the measured data. This process has been repeated ten times and the results are shown in Table S5. The significant values obtained (α>0.05) shows that null hypothesis is confirmed, measured and predicted data are related and, consequently, the model created may be enforceable.

All ten repetitions of the model include the following variables: eBC concentration before rain, swept volume and precipitation accumulated. Besides, two models also include the mean raindrop diameter. This last variable shows the greater variability.

Finally, a multi-linear regression model has been established (R^2=0.72) based on the whole data set. As expected, the model includes the three aforementioned variables, as follows:

$$\Delta eBC = (\mathrm{k_1} \cdot \mathrm{eBC_{before\ rain}}) + (\mathrm{k_2} \cdot \mathrm{Precipitation\ accumulated}) + (\mathrm{k_3} \cdot \mathrm{V_{swept}}) + \mathrm{k_4}$$

The coefficients presented the following values (± standard deviations): k_1 = -0.557 (± 0.063), k_2 = -0.0741 (± 0.007) µg m^{-3} mm^{-1}, k_3 = -3.37 10^{-11} (± 8.12 10^{-12}) µg mm^{-3} and k_4 = 0.210 (± 0.083) µg m^{-3}.

Furthermore, a multi-linear regression model has been established for ΔeBC_{ff} (R^2=0.81) and ΔeBC_{bb} (R^2=0.88).

$$\Delta eBC_{ff} = (\mathrm{k}_{1f} \cdot \mathrm{eBC_{before\ rain}}) + (\mathrm{k}_{2f} \cdot \mathrm{Precipitation\ accumulated}) + (\mathrm{k}_{3f} \cdot \mathrm{V_{swept}}) + (\mathrm{k}_{4f} \cdot \mathrm{duration}) + \mathrm{k}_{5f}$$

$$\Delta eBC_{bb} = (\mathrm{k}_{1b} \cdot \mathrm{eBC_{before\ rain}}) + (\mathrm{k}_{2b} \cdot \emptyset_{raindrop}) + \mathrm{k}_{3b}$$

The coefficients presented the following values for ΔeBC_{ff} (± standard deviations): k_{1f}= -0.598 (± 0.052), k_{2f} = 0.044 (± 0.007) µg m^{-3} mm^{-1}, k_{3f} = -6.44 10^{-11} (± 1.59 10^{-11}) µg mm^{-3}, k_{4f} = 0.056 (± 0.02) µg h^{-1} m^{-3} and k_{5f} = 0.153 (± 0.068) µg m^{-3}. For ΔeBC_{bb} the values were: k_{1b} = -0.980 (± 0.070), k_{2b} = 0.924 (± 0.379) µg m^{-3} mm^{-1} and k_{3b} = -0.194 (± 0.145) µg m^{-3}. The ΔeBC_{bb} depends more on eBC concentration before rain than ΔeBC. The ΔeBC_{ff} model includes similar variables to ΔeBC model, also incorporating the duration variable.

The model estimates the reduction in eBC well compared to the measured data (Fig. 3) becoming a valuable tool to predict the eBC behavior during rain events. Analogous representations for eBC_{ff} (Fig. S7) and eBC_{bb} (Fig. S8) are shown in Supplementary material.

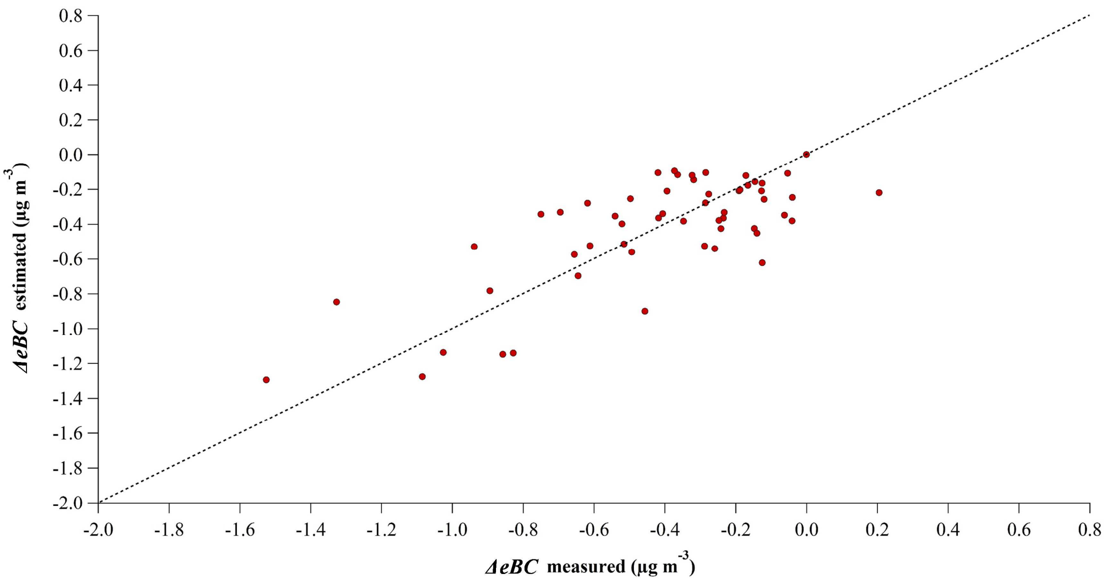

Fig. 3. ΔeBC estimated by the model vs ΔeBC measured. The dashed line (*y*=*x*) shows the perfect estimation.

4. CONCLUSIONS

We investigated BC scavenging during rain events in an urban background environment, with these main conclusions:

1. In 73% of rain events there was an effective scavenging, with a mean eBC decrease 48 ± 37% in long rain events (>8 h) and 39 ± 38% in short rain events.
2. Rain scavenging was analyzed depending on air mass origin. The air masses with a clear efficient scavenging came from Arctic (*ΔeBC%*=29 ± 21%), North Atlantic (35 ± 31%) and Saharan (18 ± 21%) areas.
3. Concerning the BC sources, the scavenging of eBC_{bb} is significantly higher compared to eBC_{ff}, probably due to the increase of its hydrophilicity because of the higher fraction of organics and a higher degree of oxygenation of biomass burning organic aerosol compared to traffic organic aerosol. Concretely, the scavenging coefficient (*SC*) mean value of eBC_{ff} for short and long rain events was $5.1\ 10^{-5}$ and $1.3\ 10^{-5}\ s^{-1}$, respectively. For eBC_{bb}, the SC values were $1.6\ 10^{-4}$ and $2.8\ 10^{-5}\ s^{-1}$ in short and long events, respectively.
4. Events with intensities higher than 2 mm h^{-1} (the maximum intensity registered in the sampling campaign was 7 mm h^{-1}) always presented an effective scavenging on eBC. However, the highest values of *SC* were recorded for rain events characterized by a low rainfall intensity and long duration. Furthermore, there was a significant positive correlation between the *SC* and the number of drops with diameters between 0.375 and 2.5 mm.
5. A linear model (R^2=0.72) was built to estimate the *ΔeBC* values with variables from weather station, aethalometer and disdrometer: eBC concentration before rain, swept volume and precipitation accumulated. A Kolmogorov-Smirnov statistical test has confirmed the goodness of fit of the model to the measured data. Finally, two other models have also been proposed to estimate the *ΔeBC* values from biomass burning and fossil fuel combustion.

One of the most important outcomes of the project is the finding that the scavenging of BC depends on the BC source (biomass burning and fossil fuel combustion). This fact could be a key factor to include in the climate models to account both the aerosol-cloud interaction and the radiative forcing caused by clouds and BC.

The combination of aethalometer-disdrometer measurements has proved to be a valuable tool for the quantification of the eBC scavenging, allowing identifying the raindrop variables that contribute to an effective scavenging of this pollutant.

FUNDINGS

This work was partially supported by the Spanish Ministry of Economy and Competitiveness (Grant TEC2014-57821-R), the University of León (Programa Propio 2015/00054/001) and the AERORAIN project (Ministry of Economy and Competitiveness, Grant CGL2014-52556-R, co-financed with FEDER funds). F. Oduber acknowledges the grant BES-2015-074473 from the Ministry of Economy and Competitiveness. C. del Blanco Alegre acknowledges the grant FPU16/05764 from the Ministry of Education, Culture and Sports.

ACKNOWLEDGEMENTS

The authors acknowledge Noelia Ramón patiently revised the final version in English. The authors gratefully acknowledge the NOAA Air Resources Laboratory (ARL) for the provision of the HYSPLIT transport and dispersion model and/or READY website (http://www.ready.noaa.gov) for the provision of the ABL data used in this study.

5. REFERENCES

Andreae, M., Ramanathan, V., 2013. Climate's dark forcings. Science (80-.). 340, 280–281.

Apte, J.S., Marshall, J.D., Cohen, A.J., Brauer, M., 2015. Addressing Global Mortality from Ambient PM2.5. Environ. Sci. Technol. 49, 8057–8066. doi:10.1021/acs.est.5b01236

Armalis, S., 1999. Wet deposition of elemental carbon in Lithuania. Sci. Total Environ. 239, 89–93. doi:10.1016/S0048-9697(99)00288-0

Becerril-Valle, M., Coz, E., Prévôt, A.S.H., Močnik, G., Pandis, S.N., Sánchez de la Campa, A.M., Alastuey, A., Díaz, E., Pérez, R.M., Artíñano, B., 2017. Characterization of atmospheric black carbon and co-pollutants in urban and rural areas of Spain. Atmos. Environ. 169. doi:10.1016/j.atmosenv.2017.09.014

Begam, G.R., Vachaspati, C.V., Ahammed, Y.N., Kumar, K.R., Babu, S.S., Reddy, R.R., 2016. Measurement and analysis of black carbon aerosols over a tropical semi-arid station in Kadapa, India. Atmos. Res. 171, 77–91. doi:10.1016/j.atmosres.2015.12.014

Bond, T.C., Doherty, S.J., Fahey, D.W., Forster, P.M., Berntsen, T., Deangelo, B.J., Flanner, M.G., Ghan, S., Kürcher, B., Koch, D., Kinne, S., Kondo, Y., Quinn, P.K., Sarofim, M.C., Schultz, M.G., Schulz, M., Venkataraman, C., Zhang, H., Zhang, S., Bellouin, N., Guttikunda, S.K., Hopke, P.K., Jacobson, M.Z., Kaiser, J.W., Klimont, Z., Lohmann, U., Schwarz, J.P., Shindell, D., Storelvmo, T., Warren, S.G., Zender, C.S., 2013. Bounding the role of black carbon in the climate system: A scientific assessment. J. Geophys. Res. Atmos. 118, 5380–5552. doi:10.1002/jgrd.50171

Budhavant, K.B., Rao, P.S.P., Safai, P.D., Leck, C., Rodhe, H., 2016. Black carbon in cloud-water and rain water during monsoon season at a high altitude station in India. Atmos. Environ. 129, 256–264. doi:10.1016/j.atmosenv.2016.01.028

Calvo, A.I., Pont, V., Olmo, F.J., Castro, A., Alados-Arboledas, L., Vicente, A.M., Fernández-Raga, M., Fraile, R., 2012. Air masses and weather types: A useful tool for characterizing precipitation chemistry and wet deposition. Aerosol Air Qual. Res. 12, 856–878. doi:10.4209/aaqr.2012.03.0068

Castro, A., Alonso-Blanco, E., González-Colino, M., Calvo, A.I., Fernández-Raga, M., Fraile, R., 2010. Aerosol size distribution in precipitation events in León, Spain. Atmos. Res. 96, 421–435. doi:10.1016/j.atmosres.2010.01.014

Cerqueira, M., Pio, C., Legrand, M., Puxbaum, H., Kasper-Giebl, A., Afonso, J., Preunkert, S., Gelencsér, A., Fialho, P., 2010. Particulate carbon in precipitation at European background sites. J. Aerosol Sci. 41, 51–61. doi:10.1016/j.jaerosci.2009.08.002

Cerully, K.M., Raatikainen, T., Lance, S., Tkacik, D., Tiitta, P., Petäjä, T., Ehn, M., Kulmala, M., Worsnop, D.R., Laaksonen, A., Smith, J.N., Nenes, A., 2011. Aerosol hygroscopicity and CCN activation kinetics in a boreal forest environment during the 2007 EUCAARI campaign. Atmos. Chem. Phys. 11, 12369–12386. doi:10.5194/acp-11-12369-2011

Chate, D.M., 2005. Study of scavenging of submicron-sized aerosol particles by thunderstorm rain events. Atmos. Environ. 39, 6608–6619. doi:10.1016/j.atmosenv.2005.07.063

Chate, D.M., Rao, P.S.P., Naik, M.S., Momin, G.A., Safai, P.D., Ali, K., 2003. Scavenging of aerosols and their chemical species by rain. Atmos. Environ. 37, 2477–2484. doi:10.1016/S1352-2310(03)00162-6

Chatterjee, A., Das, S., Ghosh, S., Raha, S., 2012. Wet scavenging of black carbon and sulphate depends on the nature of the rain; effect on the climate and global change, in: EGU General Assembly Conference Abstracts. p. 8392.

Cheng, Y.H., Liao, C.W., Liu, Z.S., Tsai, C.J., Hsi, H.C., 2014. A size-segregation method for monitoring the diurnal characteristics of atmospheric black carbon size distribution at urban traffic sites. Atmos. Environ. 90, 78–86. doi:10.1016/j.atmosenv.2014.03.023

Conrady, K., Heinke Schlünzen, K., Herber, A., 2013. Atmospheric concentration of black carbon in the western Arctic. Universität Hamburg.

Corrigan, C.E., Ramanathan, V., Schauer, J.J., 2006. Impact of monsoon transitions on the physical and optical properties of aerosols. J. Geophys. Res. Atmos. 111, 1–15. doi:10.1029/2005JD006370

Custódio, D., Cerqueira, M., Fialho, P., Nunes, T., Pio, C., Henriques, D., 2014. Wet deposition of particulate carbon to the Central North Atlantic Ocean. Sci. Total Environ. 496, 92–99. doi:10.1016/j.scitotenv.2014.06.103

Draxler, R., Rolph, G., 2012. HYSPLIT (Hybrid Single-Particle Lagrangian Integrated Trajectory). Silver Spring, MD NOAA Air Resour. Lab.

EEA, 2016. Air quality in Europe - 2016 Report. doi:10.2800/413142

EEA, 2013. Air Quality in Europe - 2013 Report. Denmark. doi:10.2800/92843

Fernández-Raga, M., Castro, A., Palencia, C., Calvo, A.I., Fraile, R., 2009. Rain events on 22 October 2006 in León (Spain): Drop size spectra. Atmos. Res. 93, 619–635. doi:10.1016/j.atmosres.2008.09.035

Font, A., Fuller, G.W., 2016. Did policies to abate atmospheric emissions from traffic have a positive effect in London? Environ. Pollut. 218, 463–474. doi:10.1016/j.envpol.2016.07.026

Fröhlich-Nowoisky, J., Kampf, C.J., Weber, B., Huffman, J.A., Pöhlker, C., Andreae, M.O., Lang-Yona, N., Burrows, S.M., Gunthe, S.S., Elbert, W., Su, H., Hoor, P., Thines, E., Hoffmann, T., Després, V.R., Pöschl, U., 2016. Bioaerosols in the Earth system: Climate, health, and ecosystem interactions. Atmos. Res. 182, 346–376. doi:10.1016/j.atmosres.2016.07.018

Gonçalves, C., Alves, C., Fernandes, A.P., Monteiro, C., Tarelho, L., Evtyugina, M., Pio, C., 2011. Organic compounds in PM2.5 emitted from fireplace and woodstove combustion of typical Portuguese wood species. Atmos. Environ. 45, 4533–4545. doi:10.1016/j.atmosenv.2011.05.071

Granat, L., Engström, J.E., Praveen, S., Rodhe, H., 2010. Light absorbing material (soot) in rainwater and in aerosol particles in the Maldives. J. Geophys. Res. Atmos. 115, 1–12. doi:10.1029/2009JD013768

Hama, S.M.L., Cordell, R.L., Kos, G.P.A., Weijers, E.P., Monks, P.S., 2017. Sub-micron particle number size distribution characteristics at two urban locations in Leicester. Atmos. Res. 194, 1–16. doi:10.1016/j.atmosres.2017.04.021

Hansen, A.D.A., 2005. Aethalometer Magee Scientific.

Hansen, A.D.A., Rosen, H., Novakov, T., 1984. The aethalometer - An instrument for the real-time measurement of optical absorption by aerosol particles. Sci. Total Environ. 36, 191–196. doi:10.1016/0048-9697(84)90265-1

Harrison, R.M., Beddows, D.C.S., Jones, A.M., Calvo, A., Alves, C., Pio, C., 2013. An evaluation of some issues regarding the use of aethalometers to measure woodsmoke concentrations. Atmos. Environ. 80, 540–548. doi:10.1016/j.atmosenv.2013.08.026

HEI Review Panel, 2013. Understanding the Health Effects of Ambient Ultrafine Particles. Heal. Eff. Inst. 122.

Hienola, A.I., Pietikäinen, J.P., Jacob, D., Pozdun, R., Petäjä, T., Hyvärinen, A.P., Sogacheva, L., Kerminen, V.M., Kulmala, M., Laaksonen, A., 2013. Black carbon concentration and deposition estimations in Finland by the regional aerosol-climate model REMO-HAM. Atmos. Chem. Phys. 13, 4033–4055. doi:10.5194/acp-13-4033-2013

ICCP, 2014. Climate Change 2014 Impacts, Adaptation, and Vulnerability Part B: Regional Aspects, Igarss 2014. doi:10.1007/s13398-014-0173-7.2

Jansen, K.L., Larson, T. V., Koenig, J.Q., Mar, T.F., Fields, C., Stewart, J., Lippmann, M., 2005. Associations between health effects and particulate matter and black carbon in subjects with respiratory disease. Environ. Health Perspect. 113, 1741–1746. doi:10.1289/ehp.8153

Janssen, N.A.H., Hoek, G., Simic-Lawson, M., Fischer, P., van Bree, L., ten Brink, H., Keuken, M., Atkinson, R.W., Anderson, H.R., Brunekreef, B., Cassee, F.R., 2011. Black Carbon as an Additional Indicator of the Adverse Health Effects of Airborne Particles Compared with PM10 and PM2.5. Environ. Health Perspect. 119, 1691–1699. doi:10.1289/ehp.1003369

Kinney, P.L., 2008. Climate Change, Air Quality, and Human Health. Am. J. Prev. Med. 35, 459–467. doi:10.1016/j.amepre.2008.08.025

Kyrö, E.M., Grönholm, T., Vuollekoski, H., Virkkula, A., Kulmala, M., Laakso, L., 2009. Snow scavenging of ultrafine particles: Field measurements and parameterization. Boreal

Environ. Res. 14, 527–538.

Laakso, L., Grönholm, T., Rannik, Ü., Kosmale, M., Fiedler, V., Vehkamäki, H., Kulmala, M., 2003. Ultrafine particle scavenging coefficients calculated from 6 years field measurements. Atmos. Environ. 37, 3605–3613. doi:10.1016/S1352-2310(03)00326-1

Ladino, L., Stetzer, O., Hattendorf, B., Günther, D., Croft, B., Lohmann, U., 2011. Experimental Study of Collection Efficiencies between Submicron Aerosols and Cloud Droplets. J. Atmos. Sci. 68, 1853–1864. doi:10.1175/JAS-D-11-012.1

Lamb, H.H., 1972. British Isles Weather Types and a Register of the Daily Sequence of Circulation Patterns 1861-1971, Geophysical memoirs. H.M. Stationery Office.

Latha, K., Badarinath, K.V.S., Manikya Reddy, P., 2005. Scavenging efficiency of rainfall on black carbon aerosols over an urban environment. Atmos. Sci. Lett. 6, 148–151. doi:10.1002/asl.108

Lelieveld, J., Evans, J.S., Fnais, M., Giannadaki, D., Pozzer, A., 2015. The contribution of outdoor air pollution sources to premature mortality on a global scale. Nature 525, 367–371. doi:10.1038/nature15371

Maria, S.F., Russell, L.M., 2005. Organic and inorganic aerosol below-cloud scavenging by suburban New Jersey precipitation. Environ. Sci. Technol. 39, 4793–4800. doi:10.1021/es0491679

Menon, S., Hansen, J., Nazarenko, L., Luo, U., 2002. Climate Effects of Black Carbon Aerosols in China and India. Science (80-.). 297, 2250–2253. doi:10.1126/science.1075159

Mori, T., Kondo, Y., Ohata, S., Moteki, N., Matsui, H., Oshima, N., Iwasaki, A., 2014. Wet deposition of black carbon at a remote site in the East China Sea 1–25. doi:10.1002/2013JD020968.Received

Novakov, T., 1984. The role of soot and primary oxidants in atmospheric chemistry. Sci. Total Environ. 36, 1–10. doi:10.1016/0048-9697(84)90241-9

Oduber, F., Castro, A., Calvo, A.I., Blanco-Alegre, C., Alonso-Blanco, E., Belmonte, P., Fraile, R., 2018. Summer-autumn air pollution in León, Spain: changes in aerosol size distribution and expected effects on the respiratory tract. Air Qual. Atmos. Heal. doi:10.1007/s11869-018-0556-6

Olszowski, T., 2015. Concentration Changes Of PM10 Under Liquid Precipitation Conditions. Ecol. Chem. Eng. S 22, 363–378. doi:10.1515/eces-2015-0019

Paramonov, M., Grönholm, T., Virkkula, A., 2011. Below-cloud scavenging of aerosol particles by snow at an urban site in Finland. Boreal Environ. Res. 16, 304–320. doi:10.1017/CBO9781107415324.004

Petzold, A., Ogren, J.A., Fiebig, M., Laj, P., Li, S.M., Baltensperger, U., Holzer-Popp, T., Kinne, S., Pappalardo, G., Sugimoto, N., Wehrli, C., Wiedensohler, A., Zhang, X.Y., 2013. Recommendations for reporting black carbon measurements. Atmos. Chem. Phys. 13, 8365–8379. doi:10.5194/acp-13-8365-2013

Pöschl, U., 2005. Atmospheric aerosols: Composition, transformation, climate and health effects. Angew. Chemie - Int. Ed. 44, 7520–7540. doi:10.1002/anie.200501122

Quinn, P., Stohl, A., Arneth, A., Berntsen, T., 2011. AMAP, 2011. The impact of black carbon on Arctic climate., Arctic Monitoring and Assessment Programme (AMAP), Oslo.

Righi, M., Klinger, C., Eyring, V., Hendricks, J., Lauer, A., Petzold, A., 2011. Climate impact of biofuels in shipping: Global model studies of the aerosol indirect effect. Environ. Sci. Technol. 45, 3519–3525. doi:10.1021/es1036157

Russo, A., Trigo, R.M., Martins, H., Mendes, M.T., 2014. NO2, PM10 and O3 urban concentrations and its association with circulation weather types in Portugal. Atmos. Environ. 89, 768–785. doi:10.1016/j.atmosenv.2014.02.010

Safai, P.D., Raju, M.P., Rao, P.S.P., Pandithurai, G., 2014. Characterization of carbonaceous aerosols over the urban tropical location and a new approach to evaluate their climatic importance. Atmos. Environ. 92, 493–500. doi:10.1016/j.atmosenv.2014.04.055

Sandradewi, J., Prévôt, A.S.H., Szidat, S., Perron, N., Alfarra, M.R., Lanz, V.A., Weingartner, E., Baltensperger, U.R.S., 2008a. Using aerosol light abosrption measurements for the quantitative determination of wood burning and traffic emission contribution to particulate matter. Environ. Sci. Technol. 42, 3316–3323. doi:10.1021/es702253m

Sandradewi, J., Prévôt, A.S.H., Weingartner, E., Schmidhauser, R., Gysel, M., Baltensperger, U., 2008b. A study of wood burning and traffic aerosols in an Alpine valley using a multi-wavelength Aethalometer. Atmos. Environ. 42, 101–112. doi:10.1016/j.atmosenv.2007.09.034

Seinfeld, J.H., Pandis, S., 2006. Atmospheric from Air Pollution to Climate Change. Atmos. Chem. Phys. 51, 1248. doi:10.1016/0016-7037(87)90252-3

Silverman, D.T., Samanic, C.M., Lubin, J.H., Blair, A.E., Stewart, P.A., Vermeulen, R., Coble, J.B., Rothman, N., Schleiff, P.L., Travis, W.D., Ziegler, R.G., Wacholder, S., Attfield, M.D., 2012. The Diesel Exhaust in Miners Study: A Nested Case-Control Study of Lung Cancer and Diesel Exhaust. JNCI J. Natl. Cancer Inst. 104, 855–868. doi:10.1093/jnci/djs034

Singh, S., Elumalai, S.P., Pal, A.K., 2016. Rain pH estimation based on the particulate matter pollutants and wet deposition study. Sci. Total Environ. 563–564, 293–301. doi:10.1016/j.scitotenv.2016.04.066

Sportisse, B., 2007. A review of parameterizations for modelling dry deposition and scavenging of radionuclides. Atmos. Environ. 41, 2683–2698. doi:10.1016/j.atmosenv.2006.11.057

Suglia, S.F., Gryparis, A., Schwartz, J., Wright, R.J., 2008. Association between traffic-related black carbon exposure and lung function among urban women. Environ. Health Perspect. 116, 1333–1337. doi:10.1289/ehp.11223

Talukdar, S., Jana, S., Maitra, A., Gogoi, M.M., 2015. Characteristics of black carbon concentration at a metropolitan city located near land-ocean boundary in Eastern India. Atmos. Res. 153, 526–534. doi:10.1016/j.atmosres.2014.10.014

Textor, C., Schulz, M., Guibert, S., Kinne, S., Balkanski, Y., Bauer, S., Berntsen, T., Berglen, T., Boucher, O., Chin, M., Dentener, F., Diehl, T., Easter, R., Feichter, H., Fillmore, D., Ghan, S., Ginoux, P., Gong, S., Grini, a., Hendricks, J., Horowitz, L., Huang, P., Isaksen, I., Iversen, T., Kloster, S., Koch, D., Kirkevåg, a., Kristjansson, J.E., Krol, M., Lauer, a., Lamarque, J.F., Liu, X., Montanaro, V., Myhre, G., Penner, J., Pitari, G., Lamarque, J.F., Liu, X., Montanaro, V., Myhre, G., Penner, J., Pitari, G., Reddy, S., Seland, Ø., Stier, P., Takemura, T., Tie, X., 2006. Analysis and quantification of the diversities of aerosol life cycles within AeroCom. Atmos. Chem. Phys. 6, 1777–1813. doi:10.5194/acpd-5-8331-2005

Tong, Z., Chen, Y., Malkawi, A., Adamkiewicz, G., Spengler, J.D., 2016. Quantifying the impact of traffic-related air pollution on the indoor air quality of a naturally ventilated building. Environ. Int. 89–90, 138–146. doi:10.1016/j.envint.2016.01.016

Tong, Z., Yang, B., Hopke, P.K., Zhang, K.M., 2017. Microenvironmental air quality impact of a commercial-scale biomass heating system. Environ. Pollut. 220, 1112–1120. doi:10.1016/j.envpol.2016.11.025

Tost, H., Jöckel, P., Kerkweg, A., Sander, R., Lelieveld, J., 2006. Technical note: A new comprehensive scavenging submodel for global atmospheric chemistry modelling. Atmos. Chem. Phys. Discuss. 5, 11157–11181. doi:10.5194/acpd-5-11157-2005

Trigo, R.M., DaCamara, C.C., 2000. Circulation weather types y their influence on the precipitation regime in Portugal. Int. J. Clim. 20, 1559–1581. doi:10.1002/1097-0088(20001115)20

UNICEF, 2016. Clear the air for children. The impact of air pollution on children. [WWW Document]. URL https://www.unicef.org/publications/index_92957.html (accessed 11.11.16).

Vejahati, F., Xu, Z., Gupta, R., 2010. Trace elements in coal: Associations with coal and minerals and their behavior during coal utilization - A review. Fuel 89, 904–911. doi:10.1016/j.fuel.2009.06.013

Virkkula, A., Mäkelä, T., Hillamo, R., Yli-Tuomi, T., Hirsikko, A., Hämeri, K., Koponen, I.K., 2007. A Simple Procedure for Correcting Loading Effects of Aethalometer Data. J. Air Waste Manage. Assoc. 57, 1214–1222. doi:10.3155/1047-3289.57.10.1214

Wang, C., Liu, H., Zhang, Y., Zou, C., Anthony, E.J., 2018. Review of arsenic behavior during coal combustion : Volatilization , transformation , emission and removal technologies. Prog. Energy Combust. Sci. 68, 1–28. doi:10.1016/j.pecs.2018.04.001

WHO, 2012. Health effects of Black carbon. Copenhagen, Denmark.

Zhang, X., Rao, R., Huang, Y., Mao, M., Berg, M.J., Sun, W., 2015. Black carbon aerosols in urban central China. J. Quant. Spectrosc. Radiat. Transf. 150, 3–11. doi:10.1016/j.jqsrt.2014.03.006

Zhang, Y., Chen, J., Yang, H., Li, R., Yu, Q., 2017. Seasonal variation and potential source regions of PM2.5-bound PAHs in the megacity Beijing, China: Impact of regional transport. Environ. Pollut. 231, 329–338. doi:10.1016/j.envpol.2017.08.025

Zhao, S., Yu, Y., He, J., Yin, D., Wang, B., 2015. Below-cloud scavenging of aerosol particles by precipitation in a typical valley city, northwestern China. Atmos. Environ. 102, 70–78. doi:10.1016/j.atmosenv.2014.11.051

Zheng, X., Zhang, S., Wu, Y., Zhang, K.M., Wu, X., Li, Z., Hao, J., 2017. Characteristics of black carbon emissions from in-use light-duty passenger vehicles. Environ. Pollut. 231, 348–356. doi:10.1016/j.envpol.2017.08.002

Zikova, N., Zdimal, V., 2016. Precipitation scavenging of aerosol particles at a rural site in the Czech Republic. Tellus B 68, 1–14. doi:10.3402/tellusb.v68.27343

Zotter, P., Herich, H., Gysel, M., El-Haddad, I., Zhang, Y., Močnik, G., Hüglin, C., Baltensperger, U., Szidat, S., Prévôt, A.S.H., 2017. Evaluation of the absorption Ångström exponents for traffic and wood burning in the Aethalometer based source apportionment using radiocarbon measurements of ambient aerosol. Atmos. Chem. Phys. 1–29. doi:10.5194/acp-17-4229-2017

Quantification of source specific black carbon scavenging using an aethalometer and a disdrometer

C. Blanco-Alegre [(1)], A.I. Calvo [(1)], E. Coz [(2)], A. Castro [(1)], F. Oduber [(1)], A.S.H. Prévôt [(3)], G. Močnik [(4)], R. Fraile [(1)]

[(1)] *Department of Physics, IMARENAB University of León, 24071 León, Spain*
[(2)] *Centre for Energy, Environment and Technology Research (CIEMAT), Department of the Environment, Madrid, Spain*
[(3)] *Laboratory of Atmospheric Chemistry, Paul Scherrer Institute, 5232 Villigen, Switzerland*
[(4)] *Condensed Matter Physics Dept., Jožef Stefan Institute, 1000 Ljubljana, Slovenia*

Corresponding Author: roberto.fraile@unileon.es +34987291543

SUPPLEMENTARY MATERIAL

1. Aethalometer model

Assuming that only these two sources exist, the total absorption coefficient $b_{abs,total}\ (\lambda)$ at wavelength λ is:

$$b_{abs,total}\ (\lambda) = b_{abs,ff}\ (\lambda) + b_{abs,bb}\ (\lambda)$$

where $b_{abs,ff}\ (\lambda)$, $b_{abs,bb}\ (\lambda)$ are the absorption coefficients of fossil fuel combustion and biomass burning, respectively.

Source apportionment of fossil fuel has been estimated through the following equations:

$$\frac{b_{abs,ff(\lambda_1)}}{b_{abs,ff(\lambda_2)}} = \left(\frac{\lambda_1}{\lambda_2}\right)^{-\mathrm{AAE_{ff}}}$$

$$\mathrm{eBC_{ff}} = \frac{b_{abs,ff(\lambda_2)}}{b_{abs,total(\lambda_2)}} \cdot\ \mathrm{eBC_{total}}(\lambda_2)$$

where $\mathrm{AAE_{ff}}$ is the absorption Ångström exponent for eBC fossil fuel.

2. Tables

Table S1. Seasonal mean values of eBC (μg m^{-3}), eBC_{ff} (μg m^{-3}) and eBC_{bb} (μg m^{-3}) measured at León during sampling (January 2016–August 2017). The values next to the mean correspond to the standard deviation.

SEASON	eBC (μg m^{-3})	eBC_{ff} (μg m^{-3})	eBC_{bb} (μg m^{-3})
Winter 2016	1.0 ± 0.9	0.8 ± 0.8	0.2 ± 0.3
Spring 2016	0.6 ± 0.5	0.5 ± 0.4	0.1 ± 0.2
Summer 2016	0.6 ± 0.5	0.6 ± 0.4	0.1 ± 0.2
Autumn 2016	1.2 ± 1.1	1.0 ± 1.0	0.2 ± 0.4
Winter 2017	1.3 ± 1.3	1.0 ± 1.2	0.4 ± 0.5
Summer 2017	0.6 ± 0.5	0.5 ± 0.3	0.1 ± 0.2

Table S2. Seasonal percentage of air masses origin (four-days before rain events).

Origin	Winter 2016	Spring 2016	Summer 2016	Autumn 2016	Winter 2017	Summer 2017	Total
Arctic	17	11	13	8	0	0	7
Atlantic	17	44	25	50	13	22	35
Continental	0	22	25	21	19	22	19
North America	0	0	0	8	6	0	3
North Atlantic	67	11	0	0	56	0	19
Saharan	0	11	38	13	6	56	17

Table S3. Rainfall characteristics and eBC variation based on Circulation Weather Types (CWTs) and air mass origin with HYSPLIT during rain events measured at León during sampling campaign. The values next to the mean correspond to the standard deviation

		N	Duration (min)	Rain (mm)	Rainfall intensity (mm h^{-1})	Wind speed (m s^{-1})	Raindrop diameter (mm)	eBC before rain (µg m^{-3})	Swept volume (mm^3 m^{-3})	*ΔeBC%*
Lamb Weather type	C	23	313	5 ± 6.8	1.52	0.9 ± 0.7	0.4 ± 0.1	0.9 ± 0.4	7.2 10^9	-1
	NW	9	173	3.4 ± 4.6	1.07	2.1 ± 1	0.3 ± 0.1	1.1 ± 0.6	3.7 10^9	-45
	N	8	98	1.4 ± 1.2	0.9	1.2 ± 0.8	0.4 ± 0.1	1.3 ± 0.6	1.4 10^9	-3
	NE	6	180	3.5 ± 4.4	1.36	0.9 ± 0.7	0.3 ± 0.2	0.9 ± 0.3	3.4 10^9	22
	W	7	266	3.6 ± 5.3	0.59	2.1 ± 1.4	0.3 ± 0.1	1.1 ± 0.4	6.5 10^9	-27
	A	5	72	0.3 ± 0.2	0.25	0.4 ± 0.3	0.3 ± 0.1	1.2 ± 0.7	5.6 10^8	27
	SW	4	120	1.2 ± 1.7	0.47	1.4 ± 0.5	0.3 ± 0.1	0.9 ± 0.4	1.5 10^9	-29
	ANW	5	108	0.9 ± 1.2	0.45	1.5 ± 1.9	0.4 ± 0.1	1.5 ± 1	1.7 10^9	-71
	CS	3	140	1.5 ± 0.2	0.92	0.5 ± 0.7	0.4 ± 0.1	1.4 ± 0.9	1.7 10^9	-38
	CW	3	240	3.4 ± 4.3	1.07	2.2 ± 2.1	0.3 ± 0.1	0.8 ± 0.2	4.7 10^9	-26
	AS	2	90	0.8 ± 0.3	0.68	1 ± 0	0.4 ± 0.1	0.6 ± 0.2	1.4 10^9	10
	AW	2	270	2.2 ± 2.6	0.38	0.8 ± 0.3	0.3 ± 0	0.9 ± 0.4	5.2 10^9	-9
	S	1	480	7.4	0.92	0.1	0.3	0.6	1.3 10^{10}	-29
	ANE	1	120	0.5	0.23	0	0.3	1	7.4 10^8	-42
	CSE	1	120	2.1	1.07	0	0.4	1.6	3.1 10^9	-65
	CSW	1	60	0.6	0.6	0.7	0.4	0.5	7.5 10^8	8
	A component	13	120	0.9 ± 1.2	0.37	0.7 ± 1.0	0.35 ± 0.08	1.2 ± 0.8	1.8 10^9	-20
	C component	30	282	4.4 ± 6.2	1.38	0.9 ± 1.0	0.36 ± 0.08	1 ± 0.5	6.3 10^9	-8
HYSPLIT model	Arctic	6	110	2.8 ± 5.9	0.86	1 ± 1.4	0.4 ± 0.1	1.1 ± 0.6	2.2 109	-29
	Atlantic	27	180	2.8 ± 3.5	1.18	1.3 ± 1.2	0.3 ± 0.1	1 ± 0.5	4.1 109	-4
	Continental	16	281	4 ± 7.5	1.16	0.9 ± 0.6	0.4 ± 0.1	1 ± 0.4	5.8 109	-6
	North America	3	120	1.3 ± 0.4	0.94	0.7 ± 0.6	0.4 ± 0	0.9 ± 0.2	1.4 109	-6
	North Atlantic	15	212	2.5 ± 3.8	0.55	1.7 ± 1.4	0.3 ± 0.1	1 ± 0.5	3.8 109	-35
	Saharan	14	210	3.4 ± 3.9	0.97	0.9 ± 0.8	0.3 ± 0.1	1.3 ± 0.8	4.6 109	-18

Table S4. Pearson correlation values between *ΔeBC%* and rain event characteristics.

	Variable	*ΔeBC%*
Rain event characteristics	Wind intensity (2 hours before rain)	**-0.348**
	Accumulated rain	**-0.225**
	Rain intensity	**-0.227**
	Event duration	**-0.242**
	Swept volume	**-0.230**
Raindrop diameter (mm)	0.125	-0.251
	0.25	-0.223
	0.375	**-0.257**
	0.5	**-0.287**
	0.75	**-0.284**
	1	**-0.281**
	1.25	**-0.278**
	1.5	**-0.276**
	1.75	**-0.269**
	2	**-0.278**
	2.5	**-0.255**
	3	-0.209
	3.5	-0.162
	4	-0.124

***Bold font indicates that the correlation is significant at 95% level.**

Table S5. Verification of the model performed (N=10), variables obtained in each N model and Kolmogorov-Smirnov (K-S) statistical test carried out between the predicted and the measured values. In N=0 was represented the model obtained with 100% of data.

N	$eBC_{before\ rain}$	V_{swept}	Precipitation accumulated	$Ø_{raindrop}$	Intercept	K-S (α)
1	-0.559	$-3.072\ 10^{-11}$	0.040	-	0.217	0.490
2	-0.559	$-3.802\ 10^{-11}$	0.044	1.126	-0.142	0.538
3	-0.636	$-2.979\ 10^{-11}$	0.036	-	0.244	0.456
4	-0.587	$-3.443 10^{-11}$	0.041	-	0.249	0.417
5	-0.639	$-2.913\ 10^{-11}$	0.039	-	0.261	0.522
6	-0.559	$-3.072\ 10^{-11}$	0.040	-	0.217	0.490
7	-0.594	$-4.228\ 10^{-11}$	0.045	-	0.276	0.569
8	-0.481	$-3.198\ 10^{-11}$	0.041	0.844	-0.112	0.621
9	-0.587	$-3.443 10^{-11}$	0.041	-	0.249	0.373
10	-0.577	$-3.381 10^{-11}$	0.041	-	0.246	0.500
0	**-0.557**	$\mathbf{-3.370\ 10^{-11}}$	**0.041**	-	**0.210**	**0.468**

3. Figures

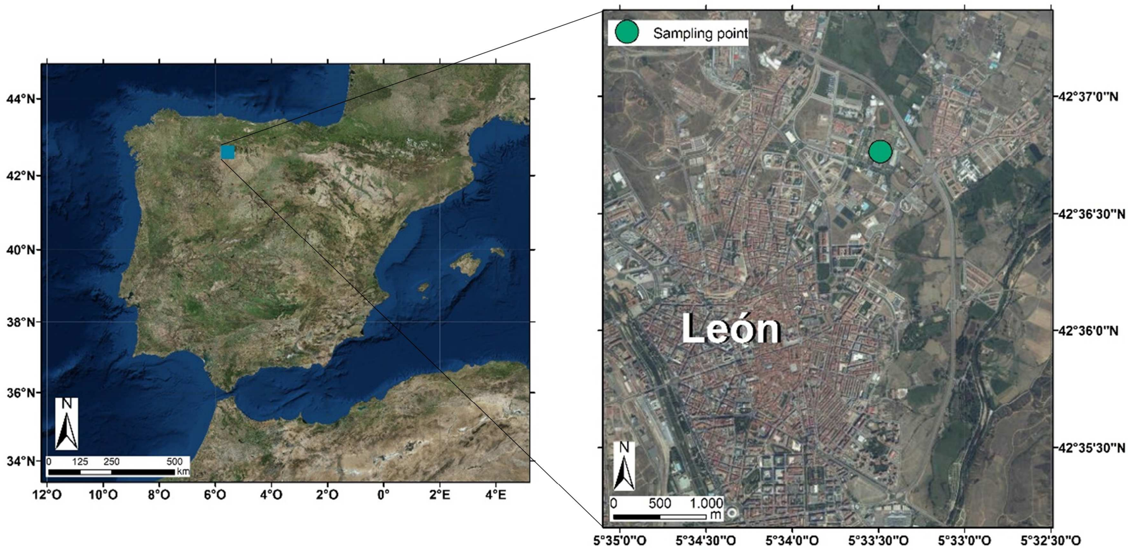

Fig. S1. León city in the NW Iberian Peninsula and the surroundings of the sampling site. Source: Earthstar Geographics, ESRI.

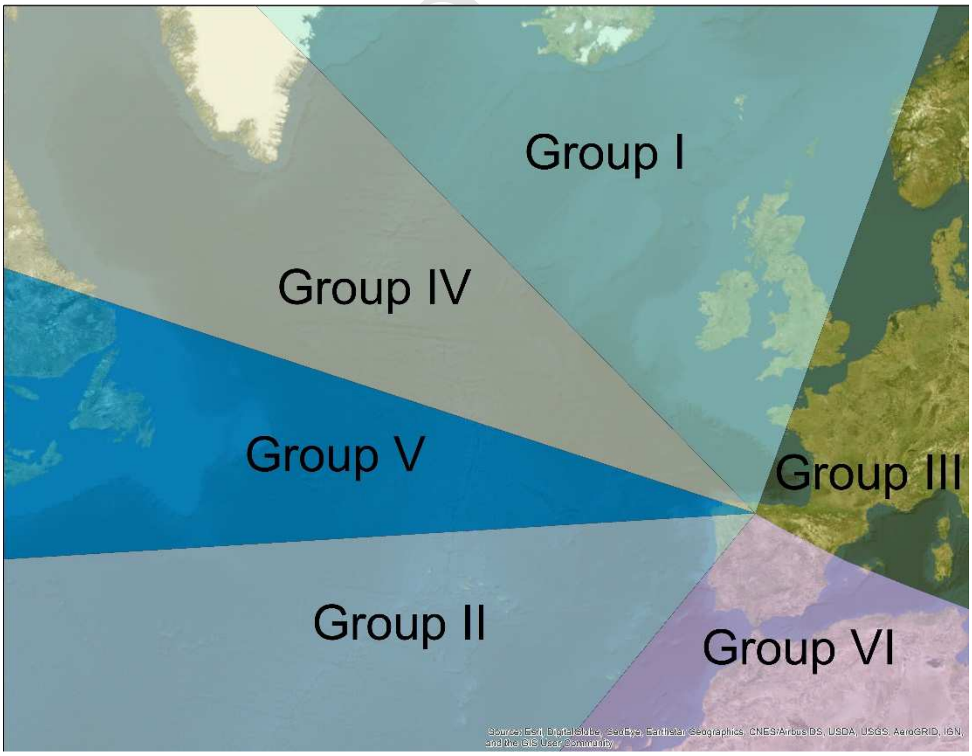

Fig. S2. Delimitation of regions for the determination of the air masses origin: I: Arctic; II: Atlantic; III: Continental; IV: North America; V: North Atlantic, and VI: Saharan.

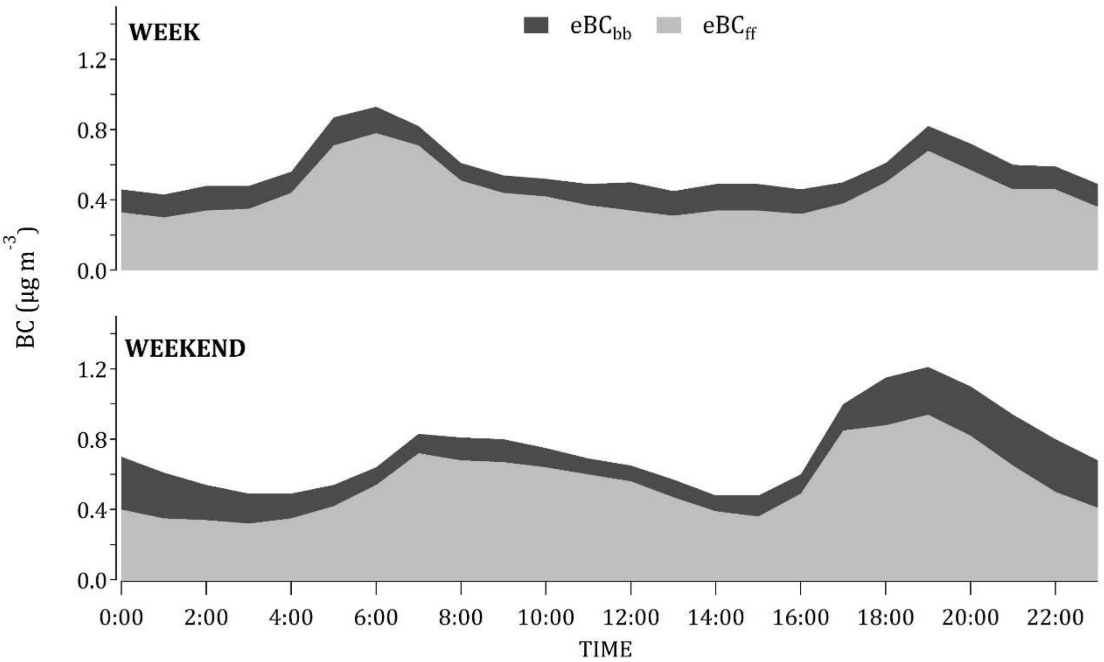

Fig. S3. Diurnal pattern of eBC_{ff} and eBC_{bb} during summer 2017.

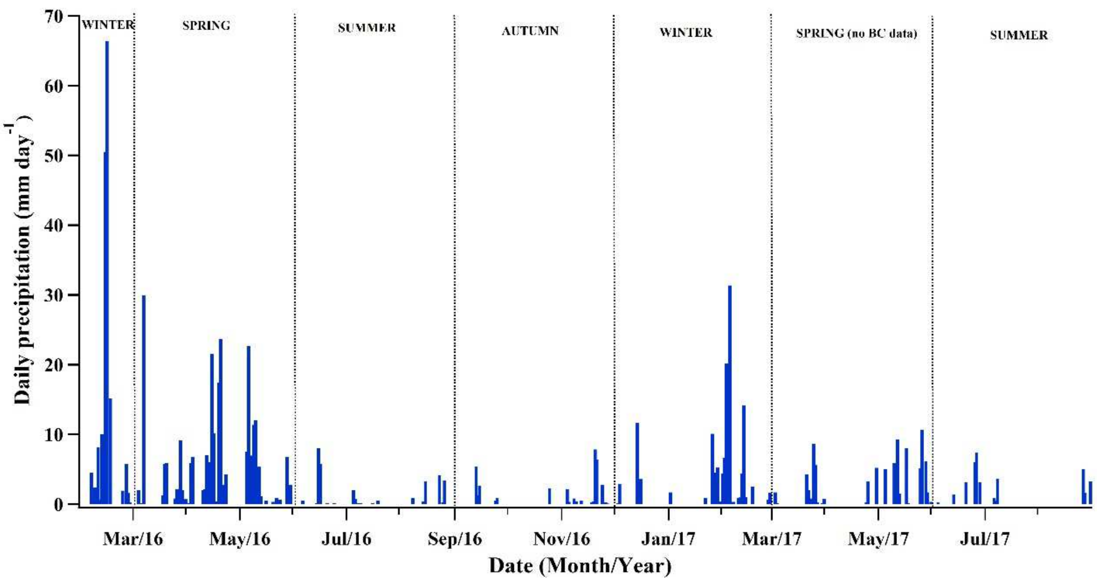

Fig. S4. Time series of rain events at León during the sampling period.

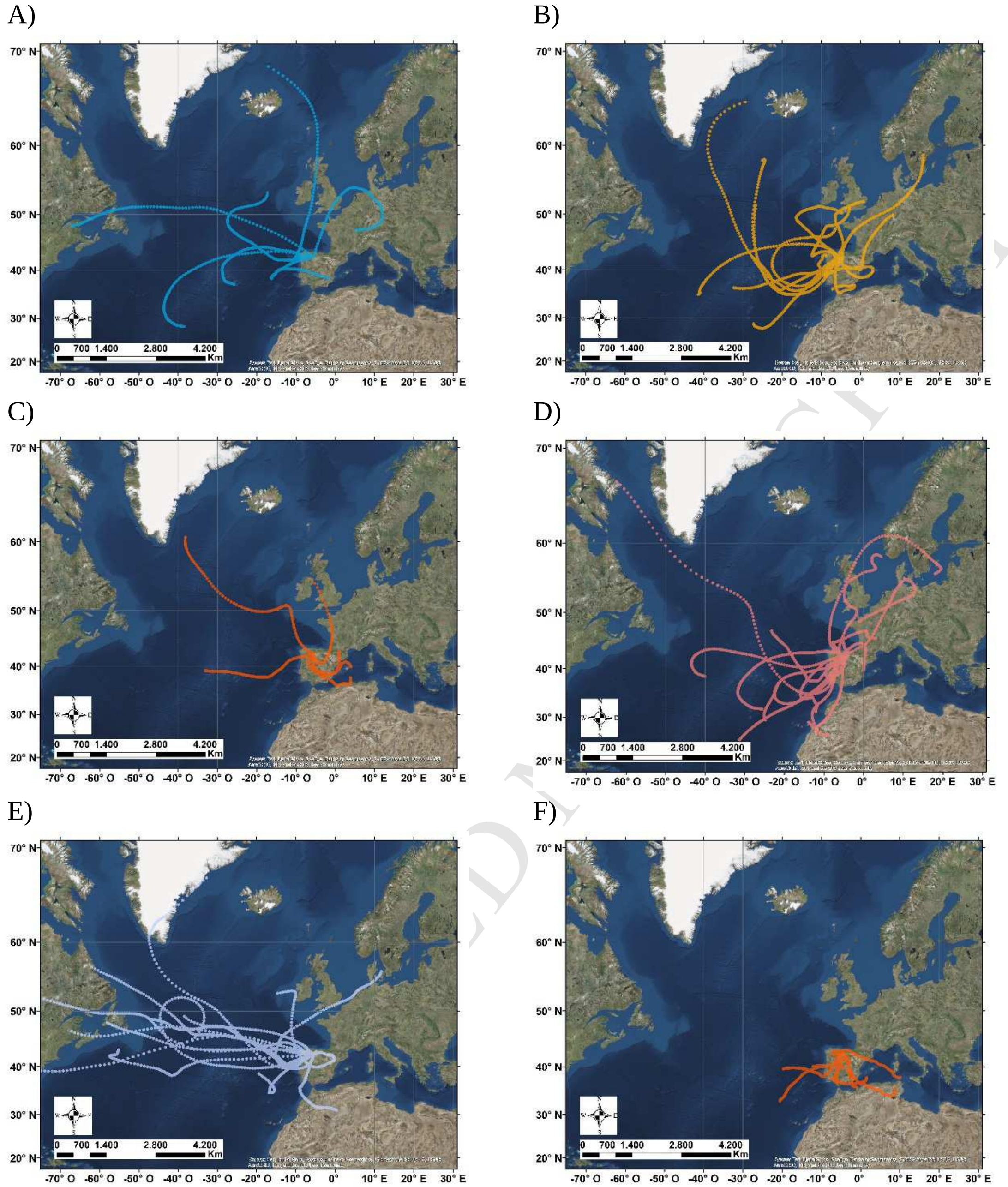

Fig. S5. Four-days back trajectories arriving at 1000 m a.g.l during rain events in León. A) Winter 2016; B) Spring 2016; C) Summer 2016; D) Autumn 2016; E) Winter 2017; F) Summer 2017.

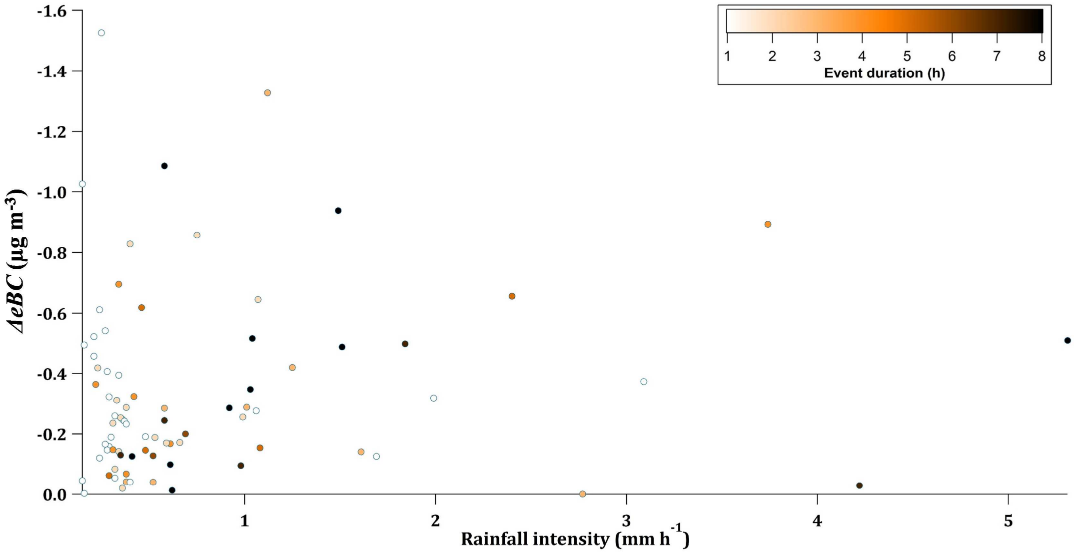

Fig. S6. *ΔeBC* as a function of rainfall intensity in events with effective scavenging. Colour dots indicate event duration (h).

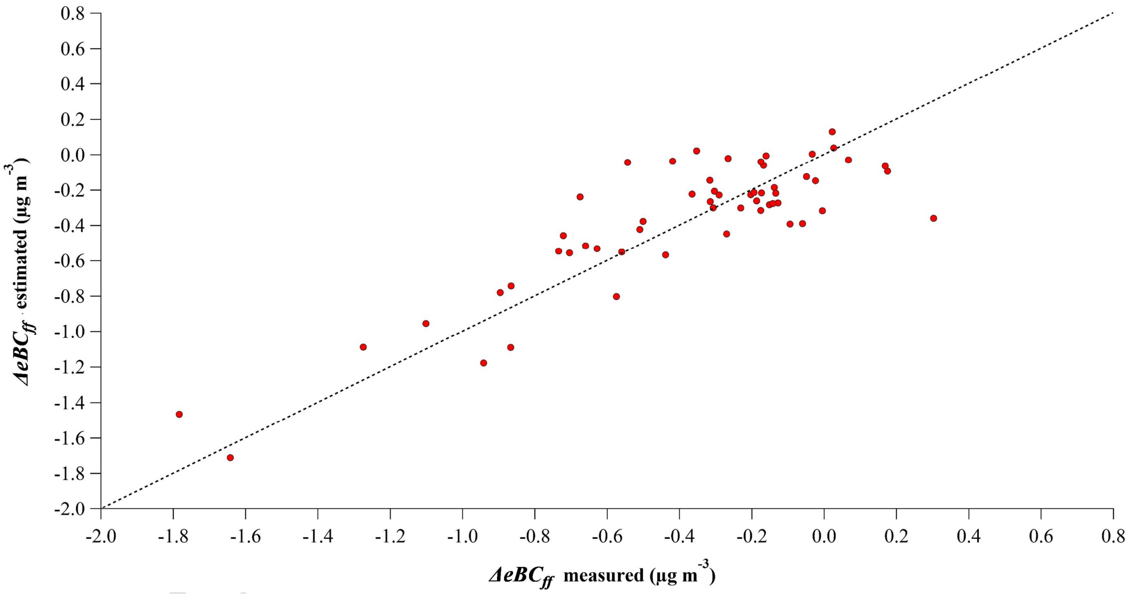

Fig. S7. ΔeBC_{ff} estimated by the model vs ΔeBC_{ff} measured. The dashed line (y=x) shows the perfect estimation.

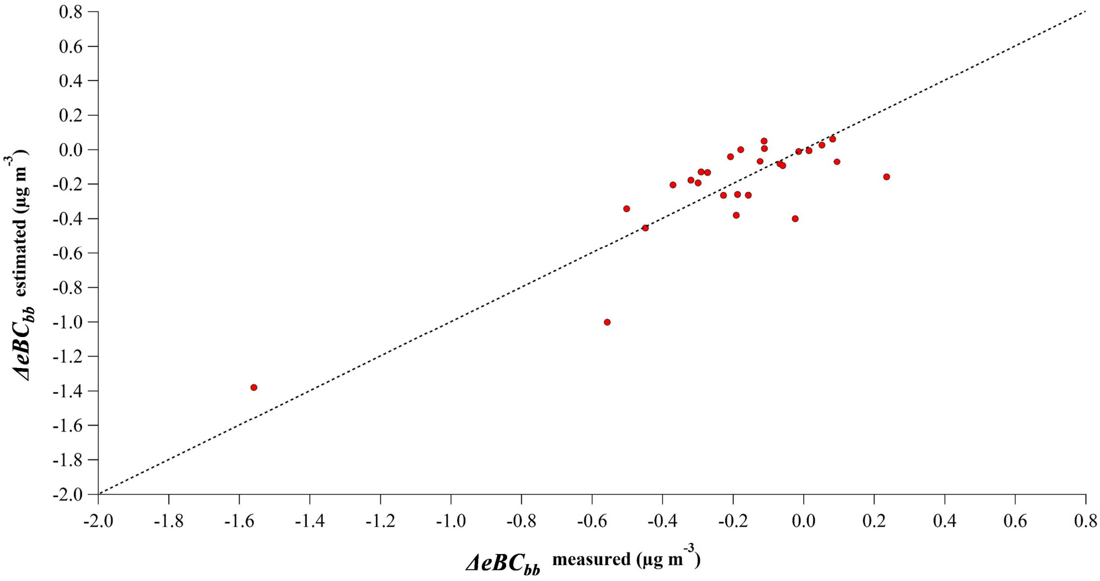

Fig. S8. ΔeBC_{bb} estimated by the model vs ΔeBC_{bb} measured. The dashed line (y=x) shows the perfect estimation.

HIGHLIGTHS

- Hourly measures were taken of black carbon and rain during 15 months in León, Spain
- 70% of the rain events showed an effective scavenging (37% eBC decrease)
- The scavenging coefficient for short rain events is 3 times the one for long events
- The scavenging was different according to specific BC source
- A model for rain scavenging of BC with aethalometer and disdrometer data was built